

BRAIDS, COMPLEX VOLUME, AND CLUSTER ALGEBRA

KAZUHIRO HIKAMI AND REI INOUE

ABSTRACT. We try to give a cluster algebraic interpretation of complex volume of knots. We construct the R-operator from the cluster mutations, and we show that it is regarded as a hyperbolic octahedron. The cluster variables are interpreted as edge parameters used by Zickert in computing complex volume.

1. Introduction

Geometrical property of quantum invariants receives renewed interests since proposed is the volume conjecture [17, 20], which suggests a relationship between the colored Jones polynomial and the hyperbolic volume of knot complements. As quantum invariants of knots such as the colored Jones polynomial are constructed by use of the Artin braid relation, it is interesting to study a hyperbolic geometrical solution of the braid relation.

A fundamental object in the 3-dimensional hyperbolic geometry is an ideal tetrahedron. When a manifold is constructed from a set of ideal tetrahedra, its complex volume, *i.e.*, a complexification of hyperbolic volume, is written in terms of the extended Rogers dilogarithm function [23]. On the other hand, the cluster algebra has been developed recently since the pioneering work [9], and there exist many applications including representation theory, Teichmüller theory, integrable systems and so on. The dilogarithm function plays an important role also in the cluster algebra [6, 22].

Purpose of this article is to give a cluster algebraic interpretation of complex volume of knots. In our previous paper [12], we gave an interpretation of the cluster mutation as a hyperbolic ideal tetrahedron, and we proposed a method to compute the complex volume of 2-bridge knots. In this article, we first give a geometric interpretation of the R-operator, which can be constructed from the cluster mutation based on a relation with the Teichmüller theory [4, 5]. We find that the R-operator in Theorem 2.3 is identified with a hyperbolic octahedron composed of four ideal tetrahedra, and that the cluster variable corresponds to an edge parameter used by Zickert [29] for a computation of complex volume. Our main claim is in Theorem 3.1 and Conjecture 3.2: following a method of Zickert, we propose a formula of complex volume in terms of cluster variables. Our construction can be naturally quantized with a help of the quantum cluster algebra [13].

This paper is organized as follows. In section 2, after explaining minimal basics of cluster algebra, we introduce the R-operator. In Section 3, we interpret the R-operator in hyperbolic geometry, and formulate the complex volume of knots at Theorem 3.1 and Conjecture 3.2. Some examples of numerical calculation are presented in section 4.

Date: April 17, 2013, revised on November 1, 2014.

Key words and phrases. knot, hyperbolic volume, complex volume, cluster algebra.

2. Cluster Algebra and Braid Relation

2.1 Cluster Variable

We briefly introduce a notion of cluster algebra used in this article. A basic reference is [9].

A cluster seed (\mathbf{x}, \mathbf{B}) is a pair of

- a cluster variable $\mathbf{x} = (x_1, \dots, x_N)$: an N -tuple of algebraically independent variables,
- an exchange matrix $\mathbf{B} = (b_{ij})$: an $N \times N$ skew symmetric integer matrix.

For each $k = 1, \dots, N$, we define the mutation μ_k of (\mathbf{x}, \mathbf{B}) by

$$\mu_k(\mathbf{x}, \mathbf{B}) = (\tilde{\mathbf{x}}, \tilde{\mathbf{B}}), \quad (2.1)$$

where

- $\tilde{\mathbf{x}} = (\tilde{x}_1, \dots, \tilde{x}_N)$ is

$$\tilde{x}_i = \begin{cases} x_i, & \text{for } i \neq k, \\ \frac{1}{x_k} \left(\prod_{j: b_{jk} > 0} x_j^{b_{jk}} + \prod_{j: b_{jk} < 0} x_j^{-b_{jk}} \right), & \text{for } i = k, \end{cases} \quad (2.2)$$

- $\tilde{\mathbf{B}} = (\tilde{b}_{ij})$ is

$$\tilde{b}_{ij} = \begin{cases} -b_{ij}, & \text{for } i = k \text{ or } j = k, \\ b_{ij} + \frac{|b_{ik}| |b_{kj}| + b_{ik} |b_{kj}|}{2}, & \text{otherwise.} \end{cases} \quad (2.3)$$

The pair $(\tilde{\mathbf{x}}, \tilde{\mathbf{B}})$ is again a cluster seed. We remark that the mutation μ_k is involutive, and that we have $\mu_j \mu_k(\mathbf{x}, \mathbf{B}) = \mu_k \mu_j(\mathbf{x}, \mathbf{B})$ if $b_{jk} = 0$.

In terms of the cluster variable \mathbf{x} , we introduce the y -variable, $\mathbf{y} = (y_1, \dots, y_N)$, defined by [10]

$$y_j = \prod_k x_k^{b_{kj}}. \quad (2.4)$$

The mutation μ_k induces a mutation of a pair (\mathbf{y}, \mathbf{B}) :

$$\mu_k(\mathbf{y}, \mathbf{B}) = (\tilde{\mathbf{y}}, \tilde{\mathbf{B}}), \quad (2.5)$$

where $\tilde{\mathbf{B}}$ is (2.3), and $\tilde{\mathbf{y}} = (\tilde{y}_1, \dots, \tilde{y}_N)$ with $\tilde{y}_j = \prod_k \tilde{x}_k^{\tilde{b}_{kj}}$ is given by

$$\tilde{y}_i = \begin{cases} y_k^{-1}, & \text{for } i = k, \\ y_i (1 + y_k^{-1})^{-b_{ki}}, & \text{for } i \neq k, b_{ki} \geq 0, \\ y_i (1 + y_k)^{-b_{ki}}, & \text{for } i \neq k, b_{ki} \leq 0. \end{cases} \quad (2.6)$$

2.2 R-operator

We set the 7 by 7 exchange matrix \mathbf{B} as

$$\mathbf{B} = \begin{pmatrix} 0 & 1 & -1 & 0 & 0 & 0 & 0 \\ -1 & 0 & 0 & 1 & 0 & 0 & 0 \\ 1 & 0 & 0 & -1 & 0 & 0 & 0 \\ 0 & -1 & 1 & 0 & 1 & -1 & 0 \\ 0 & 0 & 0 & -1 & 0 & 0 & 1 \\ 0 & 0 & 0 & 1 & 0 & 0 & -1 \\ 0 & 0 & 0 & 0 & -1 & 1 & 0 \end{pmatrix}. \quad (2.7)$$

By regarding the matrix element as

$$b_{ij} = \#\{\text{arrows from } i \text{ to } j\} - \#\{\text{arrows from } j \text{ to } i\}, \quad (2.8)$$

exchange matrix \mathbf{B} corresponds to quiver, which is dual to triangulated surface (see, *e.g.*, [8]). In our case (2.7), we have the quiver and the triangulated disk depicted in Fig. 1.

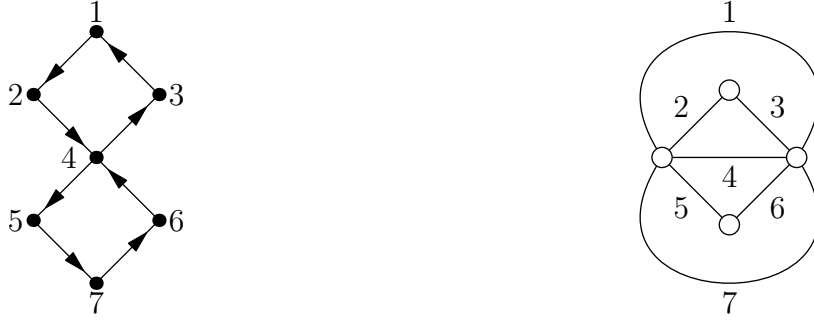


FIGURE 1. Quiver and triangulated disk

For our later use, we introduce the R-operator acting on the cluster variables associated with the quiver in Fig. 1.

Definition 2.1. We define the R-operator by

$$\mathbf{R} = s_{3,5} s_{2,5} s_{3,6} \mu_4 \mu_2 \mu_6 \mu_4. \quad (2.9)$$

Here we have used the permutation $s_{i,j}$ of subscripts i and j in seeds,

$$s_{i,j}(\dots, x_i, \dots, x_j, \dots) = (\dots, x_j, \dots, x_i, \dots).$$

Actions on the exchange matrix are defined in the same manner. Note that we have

$$\mathbf{R}^{-1} = s_{3,6} s_{2,5} s_{3,5} \mu_4 \mu_5 \mu_3 \mu_4. \quad (2.10)$$

The permutations are included in the R-operator so that the exchange matrix \mathbf{B} (2.7) is invariant under \mathbf{R} . Explicitly we have

$$\mathbf{R}^{\pm 1}(\mathbf{x}, \mathbf{B}) = (\mathbf{R}^{\pm 1}(\mathbf{x}), \mathbf{B}), \quad (2.11)$$

where

$$\begin{aligned}
 \mathbf{R}(\mathbf{x}) &= \begin{pmatrix} x_1 \\ x_5 \\ \frac{x_1 x_3 x_5 + x_3 x_4 x_5 + x_1 x_2 x_6}{x_2 x_4} \\ \frac{x_1 x_3 x_4 x_5 + x_3 x_4^2 x_5 + x_1 x_3 x_5 x_7 + x_3 x_4 x_5 x_7 + x_1 x_2 x_6 x_7}{x_2 x_4 x_6} \\ \frac{x_3 x_4 x_5 + x_3 x_5 x_7 + x_2 x_6 x_7}{x_4 x_6} \\ x_3 \\ x_7 \end{pmatrix}^{\top}, \\
 \mathbf{R}^{-1}(\mathbf{x}) &= \begin{pmatrix} x_1 \\ \frac{x_1 x_3 x_5 + x_1 x_2 x_6 + x_2 x_4 x_6}{x_3 x_4} \\ x_6 \\ \frac{x_1 x_2 x_4 x_6 + x_2 x_4^2 x_6 + x_1 x_3 x_5 x_7 + x_1 x_2 x_6 x_7 + x_2 x_4 x_6 x_7}{x_3 x_4 x_5} \\ x_2 \\ \frac{x_2 x_4 x_6 + x_3 x_5 x_7 + x_2 x_6 x_7}{x_4 x_5} \\ x_7 \end{pmatrix}^{\top}. \quad (2.12)
 \end{aligned}$$

Correspondingly, actions of the R-operator, (2.9) and (2.10), on the y -variable are respectively given as follows:

$$\mathbf{R}(\mathbf{y}) = \begin{pmatrix} \frac{y_1 (1 + y_2 + y_2 y_4)}{y_2 y_4 y_5 y_6} \\ \frac{1 + y_2 + y_6 + y_2 y_6 + y_2 y_4 y_6}{1 + y_2 + y_6 + y_2 y_6 + y_2 y_4 y_6} \\ \frac{y_2 y_4}{y_4} \\ \frac{(1 + y_2 + y_2 y_4) (1 + y_6 + y_4 y_6)}{1 + y_2 + y_6 + y_2 y_6 + y_2 y_4 y_6} \\ \frac{y_4 y_6}{y_2 y_3 y_4 y_6} \\ \frac{(1 + y_6 + y_4 y_6) y_7}{1 + y_2 + y_6 + y_2 y_6 + y_2 y_4 y_6} \end{pmatrix}^{\top},$$

$$R^{-1}(\mathbf{y}) = \left(\begin{array}{c} \frac{y_1 y_3 y_4}{1 + y_4 + y_3 y_4} \\ \frac{y_5}{1 + y_4 + y_3 y_4 + y_4 y_5 + y_3 y_4 y_5} \\ (1 + y_4 + y_3 y_4 + y_4 y_5 + y_3 y_4 y_5) y_6 \\ \frac{(1 + y_4 + y_3 y_4)(1 + y_4 + y_4 y_5)}{y_3 y_4 y_5} \\ y_2 (1 + y_4 + y_3 y_4 + y_4 y_5 + y_3 y_4 y_5) \\ \frac{y_3}{1 + y_4 + y_3 y_4 + y_4 y_5 + y_3 y_4 y_5} \\ \frac{y_4 y_5 y_7}{1 + y_4 + y_4 y_5} \end{array} \right)^T. \tag{2.13}$$

It should be remarked that the R-operator (2.9) can be also written as

$$R = s_{2,5} s_{3,6} \mu_2 \mu_6 \mu_4 \mu_2 \mu_6, \tag{2.14}$$

which can be checked from

$$\begin{aligned} s_{3,5} (\mu_3 \mu_5 \mu_4)^3 &= 1, \\ s_{2,6} (\mu_2 \mu_6 \mu_4)^3 &= 1. \end{aligned}$$

These identities correspond to a (half) periodicity in the cluster algebra associated to A_3 -type quiver, which is a sub-quiver of Fig. 1. See, *e.g.*, [9, 22].

2.3 Braid Relation

We generalize the quiver in Fig. 1 to that in Fig. 2. Therein also given is the triangulated disk, and an exchange matrix \mathbf{B} is given by the rule (2.8) as a generalization of (2.7).

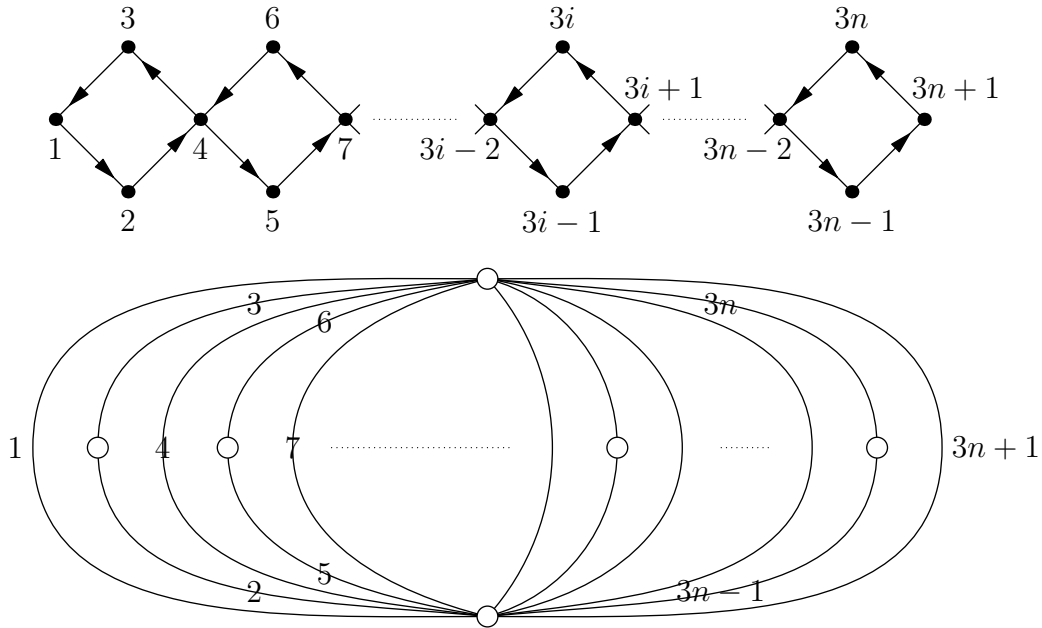


FIGURE 2. Quiver and triangulated disk.

Definition 2.2. As a generalization of (2.9), we define the R-operator $\overset{i}{\mathbf{R}}$ for $i = 1, \dots, n-1$ associated with the quiver in Fig. 2 by

$$\overset{i}{\mathbf{R}} = s_{3i,3i+2} s_{3i-1,3i+2} s_{3i,3i+3} \mu_{3i+1} \mu_{3i-1} \mu_{3i+3} \mu_{3i+1}. \quad (2.15)$$

Note that

$$\overset{i}{\mathbf{R}}^{-1} = s_{3i,3i+3} s_{3i-1,3i+2} s_{3i,3i+2} \mu_{3i+1} \mu_{3i+2} \mu_{3i} \mu_{3i+1}. \quad (2.16)$$

The exchange matrix associated to Fig. 2 is invariant under the action of the R-operators $\overset{i}{\mathbf{R}}^{\pm 1}$. The explicit forms of the actions on the cluster variable $\mathbf{x} = (x_1, x_2, \dots, x_{3n+1})$ and the y -variable $\mathbf{y} = (y_1, y_2, \dots, y_{3n+1})$ are as follows.

$$\overset{i}{\mathbf{R}}^{\pm 1}(\mathbf{x}) = (x_1, \dots, x_{3i-3}, \overset{i}{\mathbf{R}}^{\pm 1}(x_{3i-2}, \dots, x_{3i+4}), x_{3i+5}, \dots, x_{3n+1}), \quad (2.17)$$

$$\overset{i}{\mathbf{R}}^{\pm 1}(\mathbf{y}) = (y_1, \dots, y_{3i-3}, \overset{i}{\mathbf{R}}^{\pm 1}(y_{3i-2}, \dots, y_{3i+4}), y_{3i+5}, \dots, y_{3n+1}), \quad (2.18)$$

where $\overset{i}{\mathbf{R}}^{\pm 1}(x_1, \dots, x_7)$ and $\overset{i}{\mathbf{R}}^{\pm 1}(y_1, \dots, y_7)$ are defined in (2.12) and (2.13) respectively.

Theorem 2.3. *The R-operator satisfies the braid relation, namely we have*

$$\overset{i}{\mathbf{R}} \overset{i+1}{\mathbf{R}} \overset{i}{\mathbf{R}} = \overset{i+1}{\mathbf{R}} \overset{i}{\mathbf{R}} \overset{i+1}{\mathbf{R}}, \quad \text{for } i = 1, 2, \dots, n-2, \quad (2.19)$$

$$\overset{i}{\mathbf{R}} \overset{j}{\mathbf{R}} = \overset{j}{\mathbf{R}} \overset{i}{\mathbf{R}}, \quad \text{for } |i - j| > 1. \quad (2.20)$$

Proof. The second equality is trivial.

It is sufficient to check $\overset{1}{\mathbf{R}} \overset{2}{\mathbf{R}} \overset{1}{\mathbf{R}} = \overset{2}{\mathbf{R}} \overset{1}{\mathbf{R}} \overset{2}{\mathbf{R}}$ on the cluster variable (x_1, \dots, x_{10}) with the exchange matrix associated to Fig. 2 with $n = 3$. By direct computation, we can check that both actions, $\overset{1}{\mathbf{R}} \overset{2}{\mathbf{R}} \overset{1}{\mathbf{R}}$ and $\overset{2}{\mathbf{R}} \overset{1}{\mathbf{R}} \overset{2}{\mathbf{R}}$, result in the following same expressions,

$$\left(x_1, x_8, \frac{x_1 x_2 x_4 x_6 x_8 + x_1 x_3 x_5 x_7 x_8 + x_3 x_4 x_5 x_7 x_8 + x_1 x_2 x_6 x_7 x_8 + x_1 x_2 x_4 x_5 x_9}{x_2 x_4 x_5 x_7}, \right. \\ \frac{1}{x_2 x_4 x_5 x_7 x_9} \left(x_1 x_2 x_4 x_6 x_7 x_8 + x_1 x_3 x_5 x_7^2 x_8 + x_3 x_4 x_5 x_7^2 x_8 + x_1 x_2 x_6 x_7^2 x_8 + x_1 x_2 x_4 x_6 x_8 x_{10} \right. \\ \left. + x_1 x_3 x_5 x_7 x_8 x_{10} + x_3 x_4 x_5 x_7 x_8 x_{10} + x_1 x_2 x_6 x_7 x_8 x_{10} + x_1 x_2 x_4 x_5 x_9 x_{10} \right), \\ \frac{x_6 x_7 x_8 + x_6 x_8 x_{10} + x_5 x_9 x_{10}}{x_7 x_9}, \frac{x_1 x_3 x_5 + x_3 x_4 x_5 + x_1 x_2 x_6}{x_2 x_4}, \\ \left. \frac{1}{x_2 x_4 x_6 x_7 x_9} \left(x_1 x_3 x_4 x_6 x_7 x_8 + x_3 x_4^2 x_6 x_7 x_8 + x_1 x_3 x_4 x_6 x_8 x_{10} + x_3 x_4^2 x_6 x_8 x_{10} + x_1 x_3 x_4 x_5 x_9 x_{10} \right. \right. \\ \left. \left. + x_3 x_4^2 x_5 x_9 x_{10} + x_1 x_3 x_5 x_7 x_9 x_{10} + x_3 x_4 x_5 x_7 x_9 x_{10} + x_1 x_2 x_6 x_7 x_9 x_{10} \right), \right. \\ \left. \frac{x_3 x_4 x_6 x_7 x_8 + x_3 x_4 x_6 x_8 x_{10} + x_3 x_4 x_5 x_9 x_{10} + x_3 x_5 x_7 x_9 x_{10} + x_2 x_6 x_7 x_9 x_{10}}{x_4 x_6 x_7 x_9}, x_3, x_{10} \right).$$

Actions on the y -variables are induced from these actions. This completes the proof. \square

The R-operator (2.9) is not new. In [18] a solution of the Yang–Baxter equation is constructed from the quantum dilogarithm function based on a relationship with the Teichmüller theory. An operator, which has a similar action on the y -variable (2.13),

was used in studies of lamination [5]. In our case, the braiding denotes an exchange of the punctures on the disk. Also an operator which has a tropicalized action of cluster variable (2.12) was given in [4]. See [7] for applications of Teichmüller coordinates to laminations.

3. Hyperbolic Geometry

3.1 Ideal Tetrahedron

A building block of hyperbolic 3-manifold is an ideal tetrahedron whose vertices are on the boundary of a hyperbolic 3-space [25]. An ideal hyperbolic tetrahedron Δ is parameterized with cross-ratio $z \in \mathbb{C}$ of its four vertices, and the volume of Δ is given by the Bloch–Wigner function,

$$D(z) = \Im \operatorname{Li}_2(z) + \arg(1-z) \log |z|. \quad (3.1)$$

As depicted in Fig. 3, opposite edges have the same dihedral angles. Therein we have used notations,

$$z' = 1 - \frac{1}{z}, \quad z'' = \frac{1}{1-z}. \quad (3.2)$$

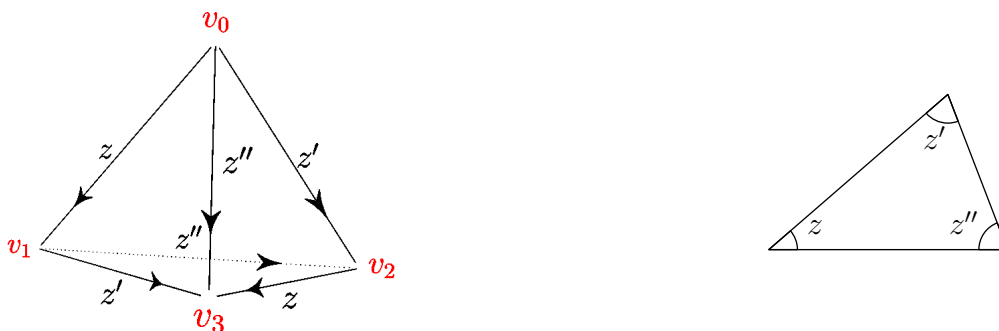


FIGURE 3. An oriented ideal tetrahedron (left), and a triangle as intersection with horosphere (right).

In case that a set of ideal tetrahedra $\{\Delta_\nu\}$ is glued faces together to a hyperbolic manifold $M = \bigcup_\nu \Delta_\nu$, the volume of M is given by

$$\operatorname{Vol}(M) = \sum_\nu D(z_\nu). \quad (3.3)$$

A complexification of $\operatorname{Vol}(M)$ known as a complex volume is defined with the Chern–Simons invariant $\operatorname{CS}(M)$. We have [23]

$$i(\operatorname{Vol}(M) + i\operatorname{CS}(M)) = \sum_\nu \operatorname{sgn}(\Delta_\nu) L([z_\nu; p_\nu, q_\nu]), \quad (3.4)$$

where $[z_\nu; p_\nu, q_\nu]$ is an element of the extended Bloch group with integers p_ν and q_ν , and $\operatorname{sgn}(\Delta_\nu)$ is $+1$ (resp. -1) when the vertex ordering of Δ_ν is same (resp. inverse) with Fig. 3. We have used the extended Rogers dilogarithm function

$$L([z; p, q]) = \operatorname{Li}_2(z) + \frac{1}{2} \log z \log(1-z) + \frac{\pi i}{2} (q \log z + p \log(1-z)) - \frac{\pi^2}{6}. \quad (3.5)$$

A method to compute p_ν and q_ν was proposed in [29]. For an oriented ideal tetrahedron of modulus z in Fig. 3, let c_{ab} be complex parameters on edge connecting vertices v_a

and v_b . Assume that they fulfill

$$\frac{c_{03} c_{12}}{c_{02} c_{13}} = \pm z, \quad \frac{c_{01} c_{23}}{c_{03} c_{12}} = \pm \left(1 - \frac{1}{z}\right), \quad \frac{c_{02} c_{13}}{c_{01} c_{23}} = \pm \frac{1}{1-z}. \quad (3.6)$$

Note that, in gluing tetrahedra together, identical edges have the same complex parameter. Then $[z; p, q]$, integers p and q for modulus z , is given by

$$\begin{aligned} \log z + p \pi i &= \log c_{03} + \log c_{12} - \log c_{02} - \log c_{13}, \\ -\log(1-z) + q \pi i &= \log c_{02} + \log c_{13} - \log c_{01} - \log c_{23}. \end{aligned} \quad (3.7)$$

Here and hereafter we mean the principal branch in the logarithm. In [29] these edge parameters c_{ab} are read from a developing map.

3.2 Octahedron

In our previous paper [12], we demonstrated that the cluster mutation can be regarded as an attachment of ideal tetrahedron to triangulated surface (see also [21]). Furthermore we claimed that the cluster variable \mathbf{x} corresponds to Zickert's complex parameters c_{ab} on edges (see [12, §2.3] for detail). Roughly speaking, this is due to that all mutations used in $\mathbb{R}^{\pm 1}(\mathbf{x})$ have a form of the Ptolemy relation, $ac + bd = ef$, which is same with (3.6).

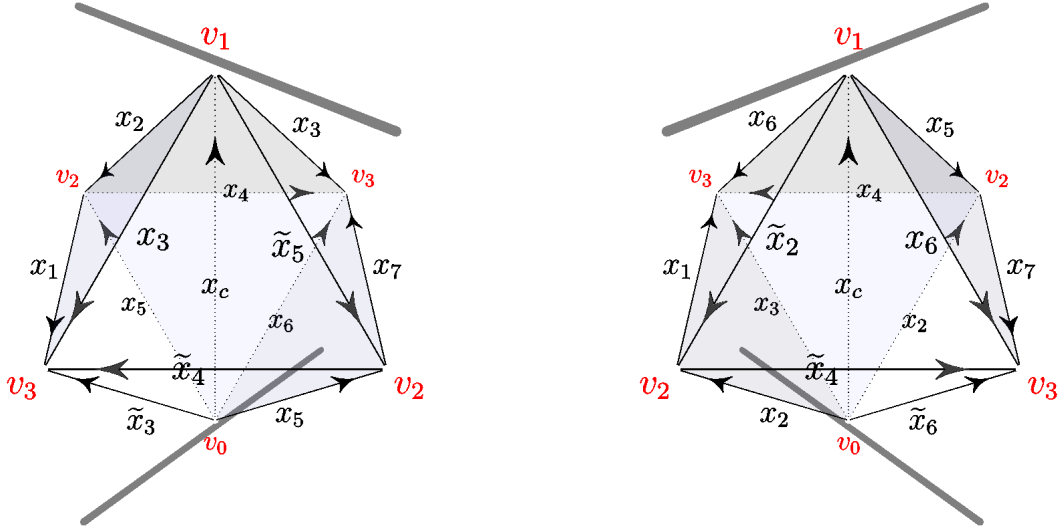


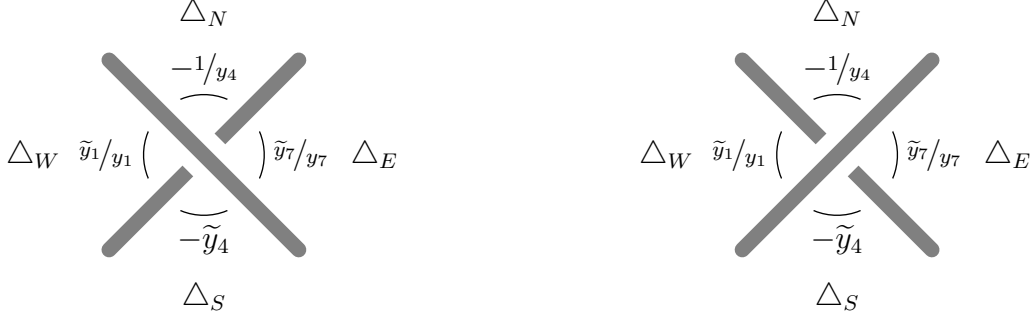
FIGURE 4. Octahedron for \mathbb{R} (left) and \mathbb{R}^{-1} (right)

For brevity, we study a case

$$\tilde{\mathbf{x}} = \mathbb{R}^{\pm 1}(\mathbf{x}).$$

Based on the observation in [12], we see that the \mathbb{R} -operator (2.9) is realized as an octahedron in Fig. 4, which is composed of four tetrahedra $\{\Delta_N, \Delta_S, \Delta_W, \Delta_E\}$. See Fig. 5 for a top view. The four tetrahedra originate from four mutations in the $\mathbb{R}^{\pm 1}$ -operator, (2.9) and (2.10); μ_2 and μ_6 in (2.9) respectively correspond to Δ_W and Δ_E , and two μ_4 's are for Δ_N and Δ_S . The cluster variables x_k and \tilde{x}_k are assigned to edges of the octahedra, and we have used

$$x_c = \frac{x_2 x_6 + x_3 x_5}{x_4}. \quad (3.8)$$

FIGURE 5. Dihedral angle at crossings, $\overset{1}{\mathbf{R}}$ (left) and $\overset{1}{\mathbf{R}}^{-1}$ (right).

Note that we have fixed vertex ordering for our convention, and that edges with the same complex parameters (*e.g.*, two pairs of edges v_0-v_2 , v_1-v_3) are identical.

As the \mathbf{R} -operator satisfies the braid relation (Theorem 2.3), we can interpret that each octahedron is assigned to every crossing of knot diagram as in Fig. 5. This reminds a fact [24] that octahedron was assigned to the Kashaev \mathbf{R} -matrix [16] (see also, [1, 3, 11, 27]). Note that another expression (2.14) of the same \mathbf{R} -operator corresponds to a decomposition of octahedron into five tetrahedra, which was used in studies of the colored Jones \mathbf{R} -matrix at root of unity [2, 24].

Δ	Volume	$\overset{1}{\mathbf{R}}$			$\overset{1}{\mathbf{R}}^{-1}$		
		$\text{sgn}(\Delta)$	z_Δ	$\frac{1}{1-z_\Delta}$	$\text{sgn}(\Delta)$	z_Δ	$\frac{1}{1-z_\Delta}$
Δ_N	$D\left(-\frac{1}{y_4}\right)$	-	$-\frac{x_2 x_6}{x_3 x_5}$	$\frac{x_3 x_5}{x_4 x_c}$	+	$-\frac{x_3 x_5}{x_2 x_6}$	$\frac{x_2 x_6}{x_4 x_c}$
Δ_S	$D(-\tilde{y}_4)$	-	$-\frac{\tilde{x}_3 \tilde{x}_5}{x_3 x_5}$	$\frac{x_3 x_5}{\tilde{x}_4 x_c}$	+	$-\frac{\tilde{x}_2 \tilde{x}_6}{x_2 x_6}$	$\frac{x_2 x_6}{x_c \tilde{x}_4}$
Δ_W	$D\left(\frac{\tilde{y}_1}{y_1}\right)$	+	$\frac{x_2 \tilde{x}_3}{x_3 x_5}$	$-\frac{x_3 x_5}{x_1 x_c}$	-	$\frac{\tilde{x}_2 x_3}{x_2 x_6}$	$-\frac{x_2 x_6}{x_1 x_c}$
Δ_E	$D\left(\frac{\tilde{y}_7}{y_7}\right)$	+	$\frac{\tilde{x}_5 x_6}{x_3 x_5}$	$-\frac{x_3 x_5}{x_c x_7}$	-	$\frac{x_5 \tilde{x}_6}{x_2 x_6}$	$-\frac{x_2 x_6}{x_c x_7}$

TABLE 1. Moduli of four tetrahedra assigned to operators $\overset{1}{\mathbf{R}}$ and $\overset{1}{\mathbf{R}}^{-1}$. Sgn “+” (resp. “-”) means that vertex ordering of tetrahedron is same (resp. inverse) with Fig. 3.

Taking into account of the vertex ordering of tetrahedra, we can determine moduli of each tetrahedron from (3.6) as in Table 1. From these results, we define dilogarithm functions for every crossing by

$$L([\overset{1}{\mathbf{R}}^{\pm 1}]; \mathbf{x}) = \sum_{t \in \{N, S, W, E\}} \text{sgn}(\Delta_t) L([z_{\Delta_t}; p_{\Delta_t}, q_{\Delta_t}]). \quad (3.9)$$

Here we have used the extended Rogers dilogarithm (3.5), and integers p_{Δ_t} and q_{Δ_t} are given from (3.7) by use of Table 1. For instance, p_{Δ_E} and q_{Δ_E} in the operator $\overset{1}{\mathbf{R}}$ are

given as

$$p_{\Delta_E} \pi i = -\log\left(\frac{\tilde{x}_5 x_6}{x_3 x_5}\right) + \log(\tilde{x}_5) + \log(x_6) - \log(x_3) - \log(x_5),$$

$$q_{\Delta_E} \pi i = -\log\left(-\frac{x_3 x_5}{x_c x_7}\right) + \log(x_3) + \log(x_5) - \log(x_c) - \log(x_7).$$

It should be remarked that, to identify the R-operator with a hyperbolic octahedron, we need a consistency condition around a central edge labeled by x_c in Fig. 4. This condition is automatically satisfied by

$$y_1 y_4 y_7 = \tilde{y}_1 \tilde{y}_4 \tilde{y}_7,$$

where $\tilde{\mathbf{y}} = \mathbf{R}^{\pm 1}(\mathbf{y})$ (2.18). In Fig. 5 denoted are dihedral angles around central axis assigned to each crossing.

The i -th braiding operator $\mathbf{R}^{\pm 1}$ in (2.15) can be interpreted in the same manner. As we have the cluster mutation $\tilde{\mathbf{x}} = \mathbf{R}^{\pm 1}(\mathbf{x})$ as in (2.17), the edge parameters (x_1, x_2, \dots, x_7) and $(\tilde{x}_1, \tilde{x}_2, \dots, \tilde{x}_7)$ in Fig. 4 are replaced respectively by $(x_{3i-2}, x_{3i-1}, \dots, x_{3i+4})$ and $(\tilde{x}_{3i-2}, \tilde{x}_{3i-1}, \dots, \tilde{x}_{3i+4})$. The moduli of the tetrahedra in Table 1 should be replaced correspondingly, and as a result we have the dilogarithm function $L([\mathbf{R}^{\pm 1}]; \mathbf{x})$ as in (3.9) by replacing x_a with x_{3i+a-3} .

3.3 Braid Group Presentation and Gluing Conditions

Our main claim is the following.

Theorem 3.1. *Let a knot K have a braid group presentation $\sigma_{k_1}^{\varepsilon_1} \sigma_{k_2}^{\varepsilon_2} \dots \sigma_{k_m}^{\varepsilon_m}$, where $\varepsilon_j = \pm 1$ and*

$$\mathcal{B}_n = \left\langle \sigma_1, \sigma_2, \dots, \sigma_{n-1} \left| \begin{array}{l} \sigma_i \sigma_j = \sigma_j \sigma_i \text{ for } |i-j| > 1 \\ \sigma_i \sigma_{i+1} \sigma_i = \sigma_{i+1} \sigma_i \sigma_{i+1} \text{ for } i = 1, 2, \dots, n-2 \end{array} \right. \right\rangle.$$

We define a cluster pattern for $\mathbf{x}[j] = (x[j]_1, \dots, x[j]_{3n+1})$ by

$$\mathbf{x}[1] \xrightarrow{\mathbf{R}^{\varepsilon_1, k_1}} \mathbf{x}[2] \xrightarrow{\mathbf{R}^{\varepsilon_2, k_2}} \dots \xrightarrow{\mathbf{R}^{\varepsilon_m, k_m}} \mathbf{x}[m+1], \quad (3.10)$$

with the exchange matrix associated to Fig. 2. We assume that the initial cluster variable $\mathbf{x}[1]$ satisfies

$$\mathbf{x}[1] = \mathbf{x}[m+1]. \quad (3.11)$$

Then the y -variables, $y[k]_i \in \mathbb{C}$, induced from the cluster pattern fulfill algebraic equations for shape parameters of ideal tetrahedra in the triangulation of $S^3 \setminus (K \cup 2\text{-points})$.

We note that the periodicity (3.11) denotes a closure of the braid, and that the 2-points are v_2 and v_3 in Fig. 4.

In the above theorem, we do not assume that a knot K is hyperbolic. We study a triangulation induced from a braid group presentation. This situation is same with the volume conjecture [17], which suggests an intimate relationship between a complex volume of $S^3 \setminus K$ and the Kashaev invariant for K defined from a quantum R -matrix.

Our triangulation is a standard one used in SnapPy [26], and the Neumann–Zagier potential function was constructed in [3] from such triangulation. See also [15], where a complex volume is studied from the same triangulation by use of quandle. So it is natural to expect that for hyperbolic knot K there exists a *geometric solution* of (3.11), where the neighbors of additional two points cancel and we endow a complete hyperbolic structure for $S^3 \setminus K$. We show in the next section numerical results for some knots, and we discuss how the cancellation of two balls occurs (see Prop. 4.1). Unfortunately, at this stage, we do not know how to extract generally such a preferable solution from (3.11). Due to that the geometric content of each octahedron is identified as in Table 1, we obtain complex volume as follows if we assume an existence of geometric solution.

Conjecture 3.2. *There exists an algebraic solution of (3.11) such that the complex volume of K is given by*

$$i(\text{Vol}(S^3 \setminus K) + i \text{CS}(S^3 \setminus K)) = \sum_{j=1}^m L(\mathbb{R}^{\varepsilon_j}; \mathbf{x}[j]). \tag{3.12}$$

See (3.9) and the end of the last subsection for the definition of the dilogarithm function $L(\mathbb{R}^{\varepsilon_j}; \mathbf{x}[j])$.

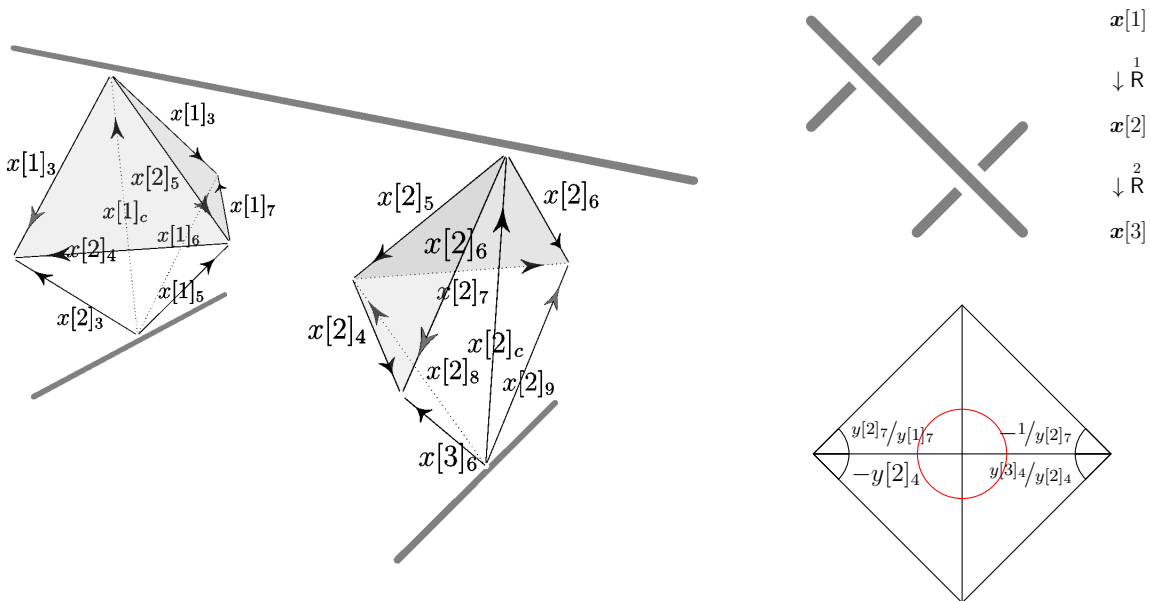


FIGURE 6. Gluing of octahedra (left) assigned to crossing (right top), and a developing map (right bottom). A consistency condition is read from a red circle.

Proof of Theorem 3.1. We need to check consistency conditions and completeness conditions as [1, 11]. We have already seen that a consistency condition around a central axis of octahedra is fulfilled. We shall check other cases. First we study a cluster pattern

$$\mathbf{x}[1] \xrightarrow{\overset{1}{R}} \mathbf{x}[2] \xrightarrow{\overset{2}{R}} \mathbf{x}[3].$$

For each crossing we assign octahedra as in Fig. 6. Therein colored faces are glued together so that identical edges have the same complex parameters. Note that (2.12)

implies $x[2]_6 = x[1]_3$ and $x[1]_7 = x[2]_7$, and that

$$x[1]_c = \frac{x[1]_2 x[1]_6 + x[1]_3 x[1]_5}{x[1]_4}, \quad x[2]_c = \frac{x[2]_5 x[2]_9 + x[2]_6 x[2]_8}{x[2]_7}.$$

Consistency condition around edge labeled by complex parameter $x[2]_5$ is checked as

$$\frac{1}{1 - \frac{y[2]_7}{y[1]_7}} \cdot \left(1 + \frac{1}{y[2]_4}\right) \cdot (1 + y[2]_7) \cdot \frac{1}{1 - \frac{y[3]_4}{y[2]_4}} = 1.$$

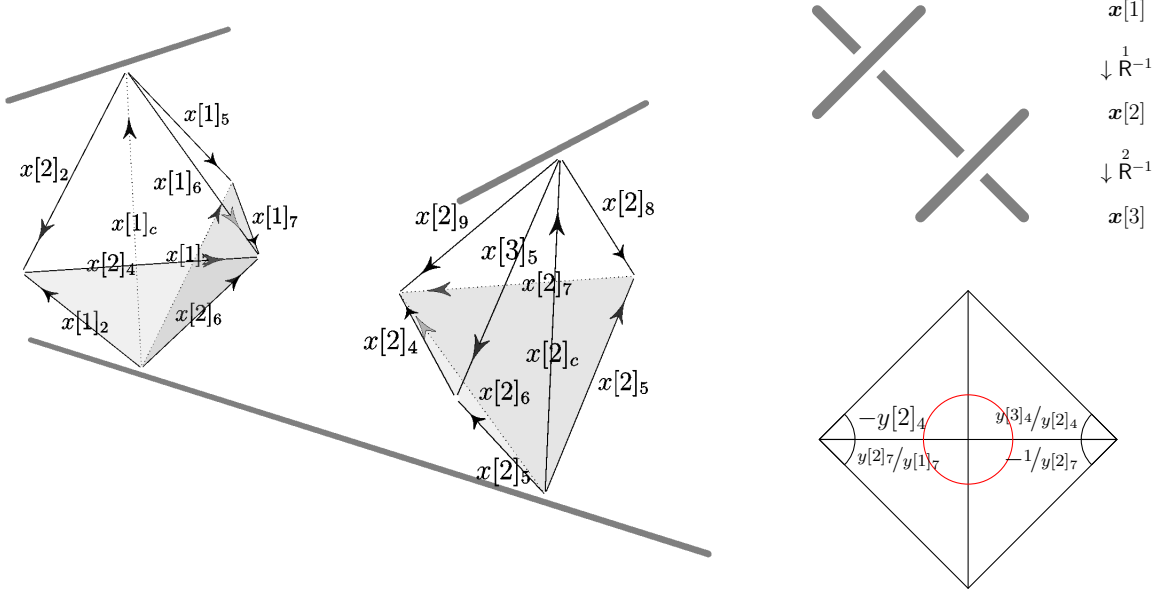


FIGURE 7. Gluing of octahedra (left) assigned to crossing (right top), and a developing map (right bottom). A consistency condition is read from a red circle.

Same is a case of a cluster pattern

$$\mathbf{x}[1] \xrightarrow{\frac{1}{\mathbb{R}^{-1}}} \mathbf{x}[2] \xrightarrow{\frac{2}{\mathbb{R}^{-1}}} \mathbf{x}[3].$$

We have octahedra as in Fig. 7, and we can check a consistency condition in the developing map as

$$\left(1 - \frac{y[1]_7}{y[2]_7}\right) \cdot \frac{1}{1 + y[2]_4} \cdot \left(1 - \frac{y[2]_4}{y[3]_4}\right) \cdot \frac{1}{1 + \frac{1}{y[2]_7}} = 1.$$

A completeness condition follows from alternating crossings. In the case that the cluster pattern is given by

$$\mathbf{x}[1] \xrightarrow{\frac{1}{\mathbb{R}}} \mathbf{x}[2] \xrightarrow{\frac{2}{\mathbb{R}^{-1}}} \mathbf{x}[3],$$

octahedra are attached to each crossing as in Fig. 8. See that identical edges have same complex parameters $x[2]_6 = x[1]_3$ and $x[1]_7 = x[2]_7$ due to (2.12). Then we can check the completeness condition as

$$\begin{aligned} \frac{1 + \frac{1}{y[2]_4}}{1 - \frac{y[2]_7}{y[1]_7}} \cdot \frac{1 + \frac{1}{y[2]_7}}{1 - \frac{y[2]_4}{y[3]_4}} &= y[1]_2 y[1]_3 \\ &= 1. \end{aligned}$$

Here the last equality follows from (2.4).

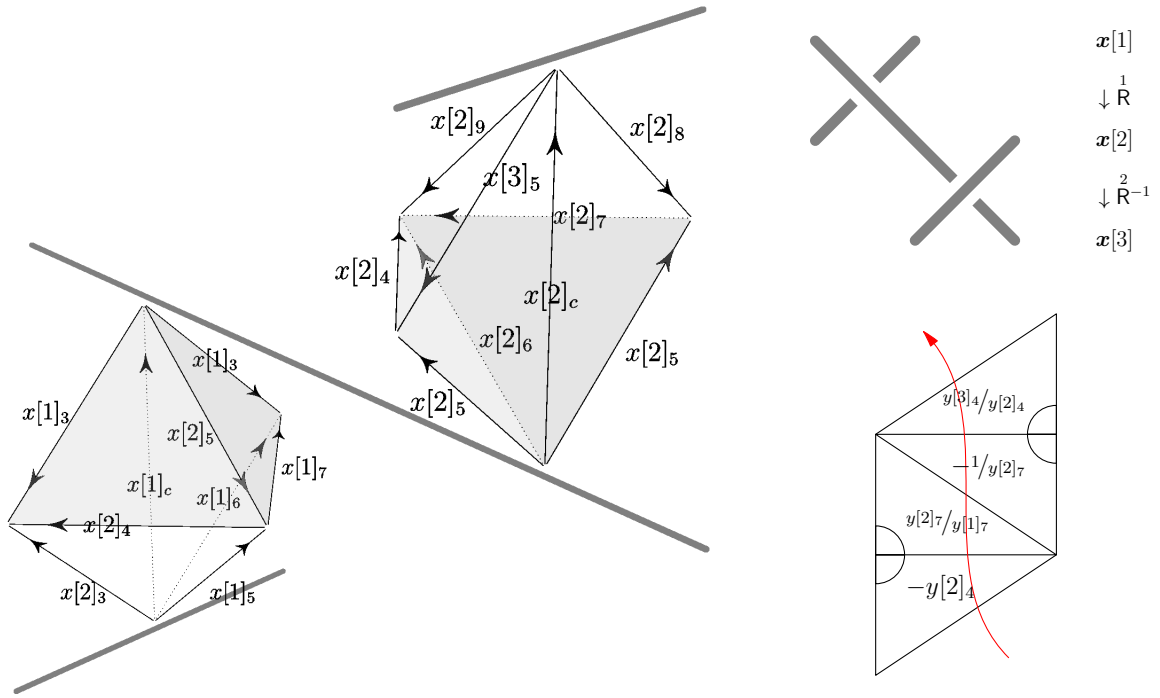


FIGURE 8. Gluing of octahedra (left) assigned to crossing (right top), and a developing map (right bottom). A completeness condition is read from a red curve.

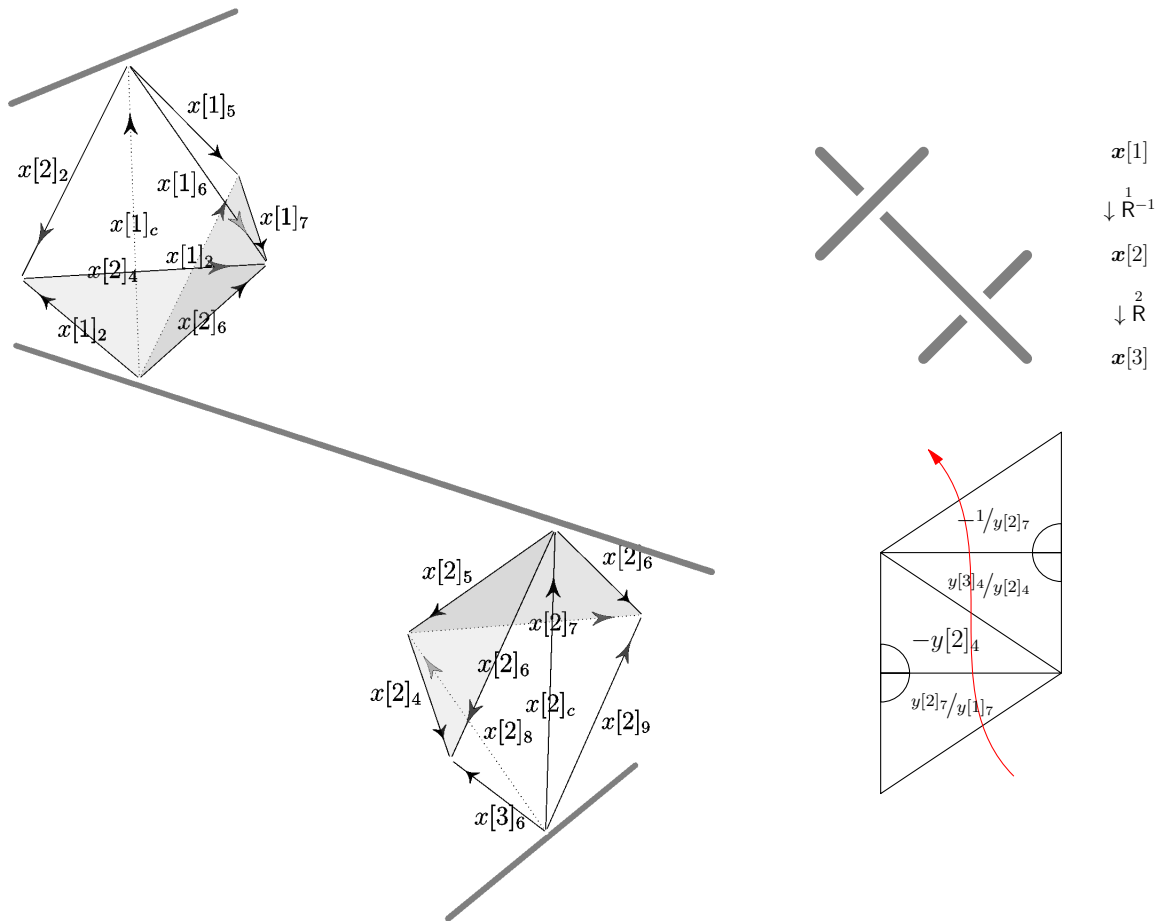


FIGURE 9. Gluing of octahedra (left) assigned to crossing (right top), and a developing map (right bottom).

We have Fig. 9 for a cluster pattern

$$\mathbf{x}[1] \xrightarrow{\overset{1}{R}^{-1}} \mathbf{x}[2] \xrightarrow{\overset{2}{R}} \mathbf{x}[3].$$

By use of (2.4), we have a completeness condition

$$\begin{aligned} \frac{1 - \frac{y[1]_7}{y[2]_7}}{1 + y[2]_4} \cdot \frac{1 - \frac{y[3]_4}{y[2]_4}}{1 + y[2]_7} &= y[1]_2 y[1]_3 \\ &= 1. \end{aligned}$$

Other cases can be checked in a similar manner, and the claim follows. \square

We note that in the above proof the completeness condition is

$$y[1]_{3i-1} y[1]_{3i} = 1, \quad \text{for } i = 1, 2, \dots, n, \quad (3.13)$$

which follows from the definition of the y -variables (2.4).

4. Examples

4.1 Figure-eight knot 4_1

We study the figure-eight knot whose braid group presentation is $\sigma_1 \sigma_2^{-1} \sigma_1 \sigma_2^{-1}$. The cluster pattern for 4_1 is thus

$$\mathbf{x}[1] \xrightarrow{\overset{1}{R}} \mathbf{x}[2] \xrightarrow{\overset{2}{R}^{-1}} \mathbf{x}[3] \xrightarrow{\overset{1}{R}} \mathbf{x}[4] \xrightarrow{\overset{2}{R}^{-1}} \mathbf{x}[5].$$

We can check that $\mathbf{x}[1] = \mathbf{x}[5]$ is fulfilled by, for example,

$$\mathbf{x}[1] = (x_1, x_2, x_2, 1, x_1 x_2, x_1^2 x_2, x_1, -x_2, -x_2, 1),$$

where $(x_1, x_2) = (e^{2\pi i/3}, 0)$. To compute the complex volume of 4_1 , we set $(x_1, x_2) = (e^{2\pi i/3} + \delta, \delta)$ with $\delta \in \mathbb{R}_{>0}$, and take a limit $\delta \rightarrow 0$ at the last. We have checked numerically that (3.12) gives $i \cdot 2 D(e^{\pi i/3}) = i \cdot 2.02988 \dots$ as desired [25].

4.2 Trefoil knot 3_1

Next example is the trefoil 3_1 , which is not hyperbolic. The braid group presentation for 3_1 is σ_1^3 , and its cluster pattern is

$$\mathbf{x}[1] \xrightarrow{\overset{1}{R}} \mathbf{x}[2] \xrightarrow{\overset{1}{R}} \mathbf{x}[3] \xrightarrow{\overset{1}{R}} \mathbf{x}[4].$$

We solve $\mathbf{x}[1] = \mathbf{x}[4]$ by choosing an initial cluster variable as

$$\mathbf{x}[1] = (x_1, x_2, x_2, 1, x_1 x_2, x_1^2 x_2, 1) \quad (4.1)$$

and get $x_1 = -\frac{1+i}{2}$ in a limit $x_2 \rightarrow 0$. We check numerically that (3.12) gives $-8.22467 \dots \simeq -\frac{5}{6}\pi^2$. It agrees with the Chern-Simons invariant of 3_1 , which is also given from asymptotic limit of the Kashaev invariant [14, 19, 28].

4.3 Interpretation of Initial Cluster Variables

In the above examples, we have singular solutions such as

$$\frac{x[1]_2}{x[1]_1}, \frac{x[1]_3}{x[1]_4} \rightarrow 0. \quad (4.2)$$

This condition for initial cluster variables denotes that a cancellation of the two additional balls occurs by connecting to the tubular neighbor of knot K as explained in [26] (see also [3]).

Proposition 4.1. *In the setting of Thm 3.1, when we set an initial cluster x -variable as (4.2), we get a canonical triangulation of $S^3 \setminus K$.*

We should note that such cancellation can occur under other choices of initial cluster variables.

Proof of Prop. 4.1. We need to connect two balls at v_2 and v_3 (see Fig. 4) to the tubular neighbor of knot K to get a triangulation of $S^3 \setminus K$. For this purpose, we introduce a triangular pillow with a pre-drilled tube as in Fig. 10. The pillow is constructed from two hyperbolic tetrahedra as in Fig. 10, and we see that there exists a drilled tube connecting two vertices (see [26]). By use of other hyperbolic tetrahedra whose vertex orderings are opposite to those in Fig. 10, we have another type of a triangular pillow as in Fig. 11.

In both Figs. 10 and 11, we assign edge parameters c_a for each edge. Shape parameters of tetrahedra are given from (3.6), and we get

$$\frac{c_3}{c_2} = 0. \quad (4.3)$$

Because of their opposite vertex orderings, a sum of the extended Rogers dilogarithm functions (3.5) for two pillows vanishes.

We insert and glue the pillow in Fig. 10 (resp. Fig. 11) to the triangular surface $x_2x_3x_4$ in Δ_N (resp. $x_1x_2x_3$ in Δ_W) in the octahedron assigned to the first crossing R . Pre-drilled tubes of the pillows connect both vertices v_2 and v_3 to v_1 in Fig. 4. To conclude, we obtain a valid triangulation of $S^3 \setminus K$. As identical edges have same edge parameters, we find that a condition (4.3) gives $\frac{x[1]_2}{x[1]_1} = \frac{x[1]_3}{x[1]_4} = 0$. \square

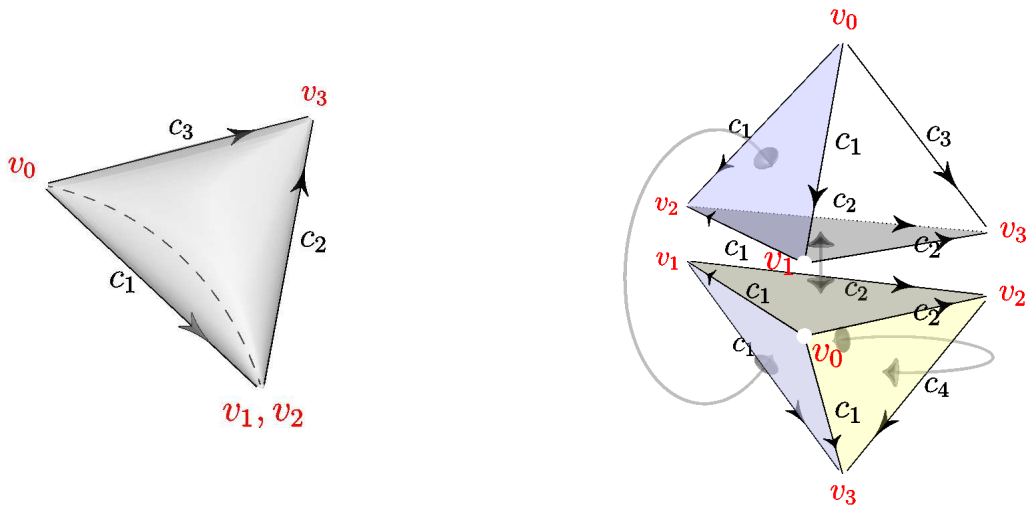


FIGURE 10. A pillow with a pre-drilled tube (left) is constructed from two ideal tetrahedra (right) by gluing colored faces together. A dashed curve denotes a tube connecting two vertices. Here c_a is an edge parameter.

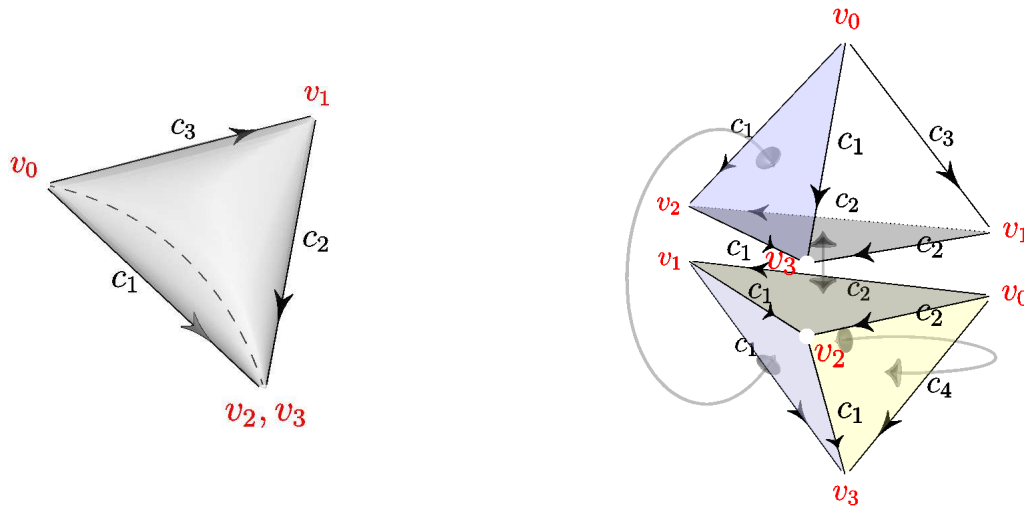


FIGURE 11. Another pillow with a pre-drilled tube (left) is given from two hyperbolic tetrahedra (right).

Acknowledgments

The authors would like to thank Jun Murakami for stimulating discussions and for comments on the manuscript. Thanks are also to Rinat Kashaev for bringing [5] to our attention. The work of KH is supported in part by JSPS KAKENHI Grant Number 23340115, 24654041. The work of RI is partially supported by JSPS KAKENHI Grant Number 22740111.

References

- [1] J. Cho, H. Kim, and S. Kim, *Optimistic limits of Kashaev invariants and complex volumes of hyperbolic links*, J. Knot Theory Ramifications **23**, 1450049 (2014) [32 pages], [arXiv:1301.6219 \[math.GT\]](#).
- [2] J. Cho and J. Murakami, *The complex volumes of twist knots via colored Jones polynomials*, J. Knot Theory Ramifications **19**, 1401–1421 (2010).
- [3] J. Cho, J. Murakami, and Y. Yokota, *The complex volumes of twist knots*, Proc. Amer. Math. Soc. **137**, 3533–3541 (2009).
- [4] P. Dehornoy, I. Dynnikov, D. Rolfsen, and B. Wiest, *Ordering Braids*, Amer. Math. Soc., Providence, 2008.
- [5] I. A. Dynnikov, *On a Yang–Baxter map and the Dehornoy ordering*, Russ. Math. Surveys **57**, 592–594 (2002).
- [6] V. V. Fock and A. B. Goncharov, *Cluster ensembles, quantization and the dilogarithm*, Ann. Sci. Éc. Norm. Supér. (4) **42**, 865–930 (2009), [arXiv:math.AG/0311245](#).
- [7] ———, *Dual Teichmüller and lamination spaces*, in A. Papadopoulos, eds., *Handbook of Teichmüller Theory Vol. 1*, pp. 647–687, Eur. Math. Soc., Zürich, 2007, [arXiv:math.DG/0510312](#).
- [8] S. Fomin, M. Shapiro, and D. Thurston, *Cluster algebras and triangulated surfaces I. cluster complexes*, Acta Math. **201**, 83–146 (2008), [arXiv:math/0608367](#).

- [9] S. Fomin and A. Zelevinsky, *Cluster algebras I. foundations*, J. Amer. Math. Soc. **15**, 497–529 (2002), [arXiv:math/0104151](#).
- [10] ———, *Cluster algebras IV: coefficients*, Composito Math. **143**, 112–164 (2007), [arXiv:math/0602259](#).
- [11] K. Hikami, *Hyperbolic structure arising from a knot invariant*, Int. J. Mod. Phys. A **16**, 3309–3333 (2001), [arXiv:math-ph/0105039](#).
- [12] K. Hikami and R. Inoue, *Cluster algebra and complex volume of once-punctured torus bundles and two-bridge knots*, J. Knot Theory Ramification **23**, 1450006 (2014) [33 pages], [arXiv:1212.6042 \[math.GT\]](#).
- [13] ———, *Braiding operator via quantum cluster algebra*, J. Phys. A: Math. Theor. **47**, 474006 (2014) [21 pages], [arXiv:1404.2009 \[math.QA\]](#).
- [14] K. Hikami and A. N. Kirillov, *Torus knot and minimal model*, Phys. Lett. B **575**, 343–348 (2003), [arXiv:hep-th/0308152](#).
- [15] A. Inoue and Y. Kabaya, *Quandle homology and complex volume*, Geom. Dedicata **171**, 265–292 (2014), [arXiv:1012.2923 \[math.GT\]](#).
- [16] R. M. Kashaev, *A link invariant from quantum dilogarithm*, Mod. Phys. Lett. A **10**, 1409–1418 (1995), [arXiv:q-alg/9504020](#).
- [17] ———, *The hyperbolic volume of knots from quantum dilogarithm*, Lett. Math. Phys. **39**, 269–275 (1997), [arXiv:q-alg/9601025](#).
- [18] ———, *On the spectrum of Dehn twists in quantum Teichmüller theory*, in A. N. Kirillov and N. Liskova, eds., *Physics and Combinatorics — Proceedings of the Nagoya 2000 International Workshop*, pp. 63–81, World Scientific, Singapore, 2001, [arXiv:math/0008148](#).
- [19] R. M. Kashaev and O. Tirkkonen, *Proof of the volume conjecture for torus knots*, Zap. Nauch. Sem. POMI **269**, 262–268 (2000), [arXiv:math/9912210](#).
- [20] H. Murakami and J. Murakami, *The colored Jones polynomials and the simplicial volume of a knot*, Acta Math. **186**, 85–104 (2001), [arXiv:math/9905075](#).
- [21] K. Nagao, Y. Terashima, and M. Yamazaki, *Hyperbolic geometry and cluster algebra*, preprint (2011), [arXiv:1112.3106 \[math.GT\]](#).
- [22] T. Nakanishi, *Periodicities in cluster algebras and dilogarithm identities*, in A. Skowronski and K. Yamagata, eds., *Representations of Algebras and Related Topics*, pp. 407–444, EMS Series of Congress Reports, European Mathematical Society (2011), [arXiv:1006.0632 \[math.QA\]](#).
- [23] W. D. Neumann, *Extended Bloch group and the Cheeger–Chern–Simons class*, Geom. Topol. **8**, 413–474 (2004), [arXiv:math/0307092 \[math.GT\]](#).
- [24] D. Thurston, *Hyperbolic volume and the Jones polynomial*, Lecture notes of École d’été de Mathématiques ‘Invariants de nœuds et de variétés de dimension 3’, Institut Fourier (1999).
- [25] W. P. Thurston, *The geometry and topology of three-manifolds*, Lecture Notes in Princeton University, Princeton (1980).
- [26] J. Weeks, *Computation of hyperbolic structures in knot theory*, in W. Menasco and M. Thistlethwaite, eds., *Handbook of Knot Theory*, pp. 461–480, Elsevier, Amsterdam, 2005, [arXiv:math/0309407 \[math.GT\]](#).

- [27] Y. Yokota, *On the complex volume of hyperbolic knots*, J. Knot Theory Ramifications **20**, 955–976 (2011).
- [28] D. Zagier, *Vassiliev invariants and a strange identity related to the Dedekind eta-function*, Topology **40**, 945–960 (2001).
- [29] C. K. Zickert, *The volume and Chern–Simons invariant of a representation*, Duke Math. J. **150**, 489–532 (2009), arXiv:0710.2049 [math.GT].

FACULTY OF MATHEMATICS, KYUSHU UNIVERSITY, FUKUOKA 819-0395, JAPAN.

E-mail address: KHikami@gmail.com

DEPARTMENT OF MATHEMATICS AND INFORMATICS, FACULTY OF SCIENCE, CHIBA UNIVERSITY, CHIBA 263-8522, JAPAN.

E-mail address: reiiy@math.s.chiba-u.ac.jp